massachusetts institute of technology — artificial intelligence laboratory

Recovering Intrinsic Images from a Single Image

Marshall F. Tappen, William T. Freeman and Edward H. Adelson

AI Memo 2002-015 September 2002

Abstract

We present an algorithm that uses multiple cues to recover shading and reflectance intrinsic images from a single image. Using both color information and a classifier trained to recognize gray-scale patterns, each image derivative is classified as being caused by shading or a change in the surface's reflectance. Generalized Belief Propagation is then used to propagate information from areas where the correct classification is clear to areas where it is ambiguous. We also show results on real images.

Acknowledgments

Portions of this work were completed while W.T.F was a Senior Research Scientist and M.F.T was a summer intern at Mitsubishi Electric Research Labs. This work was supported by an NDSEG fellowship to M.F.T, by NIH Grant EY11005-04 to E.H.A., by a grant from NTT to E.H.A., and by a contract with Unilever Research.

1 Introduction

Human beings possess the remarkable ability to interpret the causes of intensity variations in an image. The ability to differentiate the effects of shading and reflectance changes is important because, while they are both present in almost any real image, many tasks require the ability to consider the two separately. If the goal is to recover the geometry of an object, then it would be useful to have an image containing the illumination of every point in the image. Likewise, segmentation would be simpler given an image with only the reflectance at each point in the scene. Images containing only the illumination or depth of every point are known as *intrinsic images* [1] because they contain only one intrinsic characteristic of the scene being viewed.

Recovering intrinsic images is difficult because it is essentially an ill-posed problem. For any image, there are an unlimited number of possible surfaces that, combined with the right reflectance pattern, will create the input image. Therefore, we must rely on prior knowledge of the statistics of surfaces in the world to find the most likely set of intrinsic images that correspond to the scene. In this work, we are interested in two intrinsic images, the shading and reflectance image.

Most prior algorithms for finding shading and reflectance images can be broadly classified as generative or discriminative approaches. The generative approaches create possible surfaces and reflectance patterns that explain the image, then use a model to choose the most likely surface. Previous generative approaches include modeling worlds of painted polyhedra [11] or constructing surfaces from patches taken out of a training set [3]. In contrast, discriminative approaches attempt to differentiate between changes in the image caused by shading and those caused by a reflectance change. Early algorithms, such as Retinex [8], were based on simple assumptions, such as the assumption that the gradients along reflectance changes have much larger magnitudes than those caused by shading. That assumption does not hold for many real images, so recent algorithms have used more complex statistics to separate shading and reflectance. Bell and Freeman [2] trained a classifier to use local image information to classify steerable pyramid coefficients as being due to shading or reflectance. Using steerable pyramid coefficients allowed the algorithm to classify edges at multiple orientations and scales. However, the steerable pyramid decomposition has a low-frequency residual component that cannot be classified. Without classifying the low-frequency residual, only band-pass filtered copies of the shading and reflectance images can be recovered. In addition, low-frequency coefficients may not have a natural classification.

In a different direction, Weiss [13] proposed using multiple images where the reflectance is constant, but the illumination changes. This approach was able to create full frequency images, but required multiple input images of a fixed scene.

In this work, we present a system which uses multiple cues to recover full-frequency shading and reflectance intrinsic images from a single image. Our approach is discriminative, using both a classifier based on color information in the image and a classifier trained to recognize local image patterns to distinguish derivatives caused by reflectance changes from derivatives caused by shading. We also address the problem of ambiguous local evidence by using a Markov Random Field to propagate the classifications of those areas where the evidence is clear to those where it is not.

2 Separating Shading and Reflectance

Our algorithm separates shading from reflectance by classifying each image derivative as being caused by shading or a reflectance change. We assume that the input image, $\mathcal{I}(x, y)$, can be expressed as the product of the shading image, $\mathcal{S}(x, y)$, and the reflectance image, $\mathcal{R}(x, y)$. Considering the images in the log domain, the derivatives of the input image are the sum of the derivatives of the shading and reflectance images. It is unlikely that significant shading boundaries and reflectance edges occur at the same point, thus we make the simplifying assumption that every image derivative is either caused by shading or reflectance. This reduces the problem of specifying the shading and reflectance derivatives to that of binary classification of the image's x and y derivatives.

Labelling each x and y derivative produces estimates of the derivatives of the shading and reflectance images. Each derivative represents a set of linear constraints on the image and using both derivative images results in an over-constrained system. We recover each intrinsic image from its derivatives by using the method introduced by Weiss in [13] to find the pseudo-inverse of the over-constrained system of derivatives. If f_x and f_y are the filters used to compute the x and y derivatives and $\mathcal{F}_x$ and $\mathcal{F}_y$ are the estimated derivatives of shading image, then the shading image, $\mathcal{S}(x, y)$ is:

$$\mathcal{S}(x, y) = g \star [(f_x(-x, -y) \star \mathcal{F}_x) + (f_y(-x, -y) \star \mathcal{F}_y)] \tag{1}$$

where $\star$ is convolution, $f(-x, -y)$ is a reversed copy of $f(x, y)$, and g is the solution of

$$g \star [(f_x(-x, -y) \star f_x(x, y)) + (f_y(-x, -y) \star f_x(x, y))] = \delta \tag{2}$$

The reflectance image is found in the same fashion. One nice property of this technique is that the computation can be done using the FFT, making it more computationally efficient.

3 Classifying Derivatives

With an architecture for recovering intrinsic images, the next step is to create the classifiers to separate the underlying processes in the image. Our system uses two classifiers, one which uses color information to separate shading and reflectance derivatives and a classifier for gray-scale images.

3.1 Using Color Information

Our system takes advantage of the property that changes in color between pixels indicate a reflectance change [10]. When surfaces are diffuse, any changes in a color image due to shading should affect all three color channels proportionally. Assume two adjacent pixels in the image have values $\mathbf{c}_1$ and $\mathbf{c}_2$, where $\mathbf{c}_1$ and $\mathbf{c}_2$ are RGB triplets. If the change between the two pixels is caused by shading, then $\mathbf{c}_2 = \alpha\mathbf{c}_1$ for some scalar α. Intuitively, shading should only cause the intensity of surface's color to change, not the chromaticity.

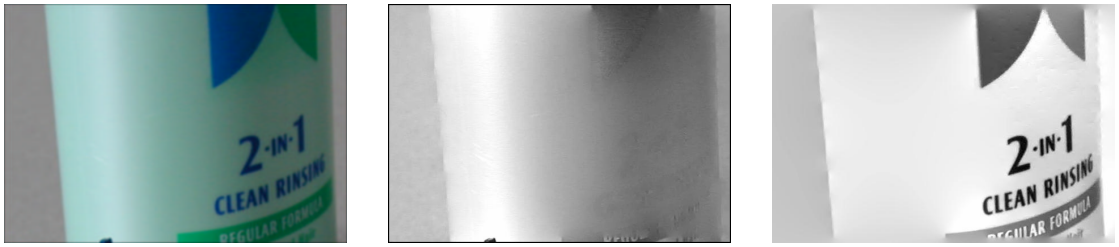

(a) Original Image (b) Shading Image (c) Reflectance Image

Figure 1: Example. Computed using Color Detector. To facilitate printing, the intrinsic images have been computed from a gray-scale version of the image. The color information is used solely for classifying derivatives in the gray-scale copy of the image.

To measure the likelihood that a color change is caused by a reflectance change, we treat each RGB triplet as a vector and normalize them to create $\hat{\mathbf{c}}_1$ and $\hat{\mathbf{c}}_2$. We then use the angle between $\hat{\mathbf{c}}_1$ and $\hat{\mathbf{c}}_2$ to find reflectance changes. When the change is caused by shading, $(\hat{\mathbf{c}}_1 \cdot \hat{\mathbf{c}}_2)$ equals 1. If $(\hat{\mathbf{c}}_1 \cdot \hat{\mathbf{c}}_2)$ is below a threshold, then the derivative associated with the two colors is classified as a reflectance derivative. Using only the color information, this approach is similar to that used in [6]. The primary difference is that our system classifies the vertical and horizontal derivatives independently.

Figure 1 shows an example of the results produced by the algorithm. The classifier marked all of the reflectance areas correctly and the text is cleanly removed from the bottle. This example also demonstrates the high quality reconstructions that can be obtained by classifying derivatives.

3.2 Using Gray-Scale Information

While color information is useful, the assumptions of the color-based classifier will not always hold. In addition, the statistics of surfaces and illumination often provide enough information to separate shading and reflectance from gray-scale information alone. In this section, we describe how to classify image derivatives using color information.

The basic feature of our classifier is the absolute value of the response of a linear filter. We refer to a feature computed in this manner as a *non-linear filter*. The output of a non-linear, F, given an input patch I_p is

$$F = |I_p \star w| \tag{3}$$

where $\star$ is convolution and w is a linear filter. The filter, w is the same size as the image patch, I, and we only consider the response at the center of I_p. This makes the feature a function from a

(a) Original Image (b) Shading Image (c) Reflectance Image

Figure 2: Results obtained using the gray-scale classifier.

patch of image data to a scalar response. This feature could also be viewed as the absolute value of the dot product of I_p and w.

We chose to use the responses of linear filters as the basis for our feature, in part, because they have been used successfully for characterizing [9] and synthesizing [7] images of textured surfaces. Another advantage of using linear filters is that once specific filters are chosen as features for the classifier, it should be relatively simple to interpret what image patterns the feature is responding to. Using the absolute value of the filter response is necessary because we are only interested in the magnitude of the response, not the sign. Changing an edge from a dark to light transition into a light to dark transition should not change its classification.

The non-linear filters are used to classify derivatives with a classifier similar to that used by Tieu and Viola in [12]. This classifier uses the AdaBoost [4] algorithm to combine a set of weak classifiers into a single strong classifier. In our implementation, each weak classifier is a threshold test on the output of one non-linear filter. The linear filter in each weak classifier are chosen greedily. At each iteration, the learning algorithm chooses the linear filter that best classifies the training set from a set of oriented first and second derivative of Gaussian filters.

The training set consists of a mix of images of rendered fractal surfaces and images of shaded ellipses placed randomly in the image. Examples of reflectance changes were created using images of random lines and images of random ellipse painted onto the image. Examples can be seen in Figure 3. In the training set, the illumination is always coming from the right side of the image. When evaluating test images, the classifier will assume that the test image is also lit from the right.

Figure 2 shows the results of the gray-scale classifier. The grafitti paint and the rock surface are separated into reflectance and shading images, respectively. Some shading changes in the upper

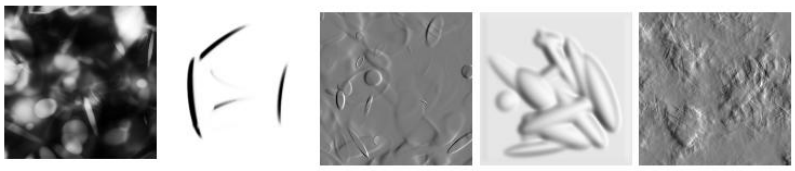

Figure 3: Example images from the training set. The first two are examples of reflectance changes and the last three are examples of shading

right corner of the image have been mistakenly classified as reflectance changes, likely due to the shading training set not containing strong ridges such as those in the image.

The examples shown are computed without taking the log of the input image before processing it. The input images are uncalibrated and ordinary photographic tonescale is very similar to a log transformation. Errors from not taking log of the input image first would cause one intrinsic image to modulate the local brightness of the other. However, this does not occur in the results.

4 Propagating Evidence

While the classifier works well, there are still areas in the image where the local information is ambiguous. An example of this is shown in Figure 4. Locally, the center of the mouth area is similar in appearance to the side of an ellipse that points away from a light source. This causes the derivatives around the mouth to be classified with low certainty. However, the corners of the mouth can be classified as being caused by a reflectance change with little ambiguity. A mechanism is needed to propagate information from the corners of the mouth, where the classification is clear, into areas where the local evidence is ambiguous. This will allow areas where the classification is clear to disambiguate those areas where it is not. Intuitively, we want points on the same contour to share the same classification.

In order to propagate evidence, we treat each derivative as a node in a Markov Random Field with two possible states, indicating whether the derivative is caused by shading or caused by a reflectance change. Setting the compatibility functions between nodes correctly will force nodes along the same contour to have the same classification.

4.1 Model for the Potential Functions

The compatibility functions in the MRF are set to only constrain whether two neighboring nodes must have the same value or not. Each potential function,$\psi(x_i, x_j)$ has two possible values, one when $x_i = x_j$ and one when $x_i \neq x_j$. Each $\psi(\cdot)$ should be set to have a high compatibility when $x_i = x_j$ and both x_i and x_j are along a contour. This dependence on the image can be expressed by defining the compatibility function $\psi_0(\mathcal{I})$ as the compatibility when the two nodes have a different value and $\psi_1(\mathcal{I})$ to be the compatibility when the nodes have the same value. Each ψ has been

(a) (b) (c)

Figure 4: An example where propagation is needed. (a) The original image (b) Vertical derivatives where the certainty of the classification from shape information is greater than 60% are marked in white. Notice how the center of the mouth is ambiguous. (c) The certainty after information has been propagated. The remaining black points are still ambiguous after propagation because they are not on an image contour.

written as a function of the input image, $\mathcal{I}$ because the strength of the compatibility is dependent upon whether there is a contour in the image near the location of ψ.

To simplify learning the potential functions, $\psi_1(\mathcal{I})$ is set to $1 - \psi_0(\mathcal{I})$ with $\psi_0(\mathcal{I})$ constrained to be between 0 and 1. This constraint is fulfilled by specifying that $\psi_0(\mathcal{I}) = g(z(\mathcal{I}))$, where $g(\cdot)$ is the logistic function and $z(\mathcal{I})$ corresponds to how necessary it is for two neighboring nodes to have the same value.

4.2 Learning the Potential Functions

In order to learn $z(\mathcal{I})$ we choose a set of image features that reflect our heuristics about how objects should be grouped. In this work, we used two local image features, the magnitude of the image and the difference in orientation between the gradient and the orientation of the graph edge. Using these measures reflect our heuristic that derivatives along contours should have the same value.

The difference in orientation between a horizontal graph edge and image contour, $\hat{\phi}$, is found from the orientation of the image gradient, ϕ. Assuming that $-\pi/2 \leq \phi \leq \pi/2$, the angle between a horizontal edge and the image gradient,$\hat{\phi}$, is $\hat{\phi} = |\phi|$. For vertical edges, $\hat{\phi} = |\phi| - \pi/2$.

To find the values of $z(\cdot)$ we maximize the probability of a set training examples over the parameters of $z(\cdot)$. The probability of each training sample is

$$P = \frac{1}{Z} \prod_{(i,j)|x_i \neq x_j} \psi_0(\mathcal{I}) \prod_{(i,j)|x_i = x_j} \psi_1(\mathcal{I}) \tag{4}$$

where all (i, j) are the indices of neighboring nodes in the MRF and Z is a normalization constant.

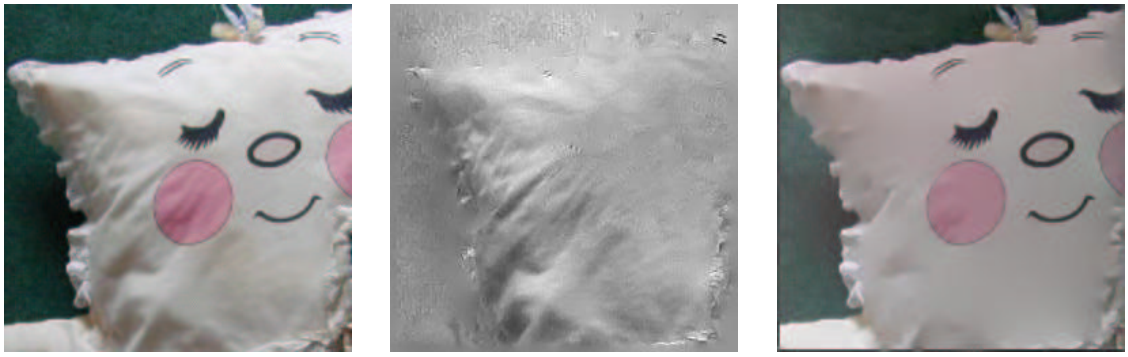

(a) Original Image (b) Shading Image (c) Reflectance Image

Figure 5: The pillow from Figure 4. This is found by combining the local evidence from the color and gray-scale classifiers, then using Generalized Belief Propagation to propagate local evidence.

The function relating the image features to ψ, $z(\cdot)$, is set to be a linear function and are found by maximizing equation 4 over a set of training images similar to those used to train the local classifier. In order to simplify the training process, we approximate the true probability of each MRF by assuming that Z is constant. Doing so leads to the following value of $z(\cdot)$:

$$z(\hat{\phi}, |\nabla \mathcal{I}|) = -1.2 \times \hat{\phi} + 1.62 \times |\nabla \mathcal{I}| + 2.3 \tag{5}$$

where $|\nabla \mathcal{I}|$ is magnitude of the image gradient and both $\hat{\phi}$ and $|\nabla \mathcal{I}|$ have been normalized to be between 0 and 1. These measures break down in areas with a weak gradient, so we set $z(\cdot)$ to 0.5 for regions of the image with a gradient magnitude less than 0.05.

Larger values of $z(\cdot)$ correspond to a belief that the derivatives connected by the edge should have the same value, while negative values signify that the derivatives should have a different value. The values in equation 5 correspond with our expected results; two derivatives are constrained to have the same value when they are along an edge in the image that has a similar orientation to the edge in the MRF connecting the two nodes.

4.3 Inferring the Correct Labelling

Once the compatibility functions have been learned, the label of each derivative can be inferred. The local evidence for each node in the MRF is obtained from the results of the color classifier and from the gray-scale classifier by assuming that the two are statistically independent. It is necessary to use the color information because propagation cannot help in areas where the gray-scale classifier misses an edge altogether. In Figure 5, the cheek patches on the pillow, which are pink in the color image, are missed by the gray-scale classifier, but caught by the color classifier. For the results

(a) Original Image (b) Shading Image (c) Reflectance Image

Figure 6: Example generated by combining color and gray-scale information, along with using propagation.

shown, we used the results of the AdaBoost classifier to classify the gray-scale images and used the method suggested by Friedman et al. to obtain the probability of the labels [5].

We used the Generalized Belief Propagation algorithm [14] to infer the best label of each node in the MRF because ordinary Belief Propagation performed poorly in areas with both weak local evidence and strong compatibility constraints. The results of using color, gray-scale information, and propagation can be seen in Figure 5. The ripples on the pillow are correctly identified as being caused by shading, while the face is correctly identified as having been painted on. Figure 6 contains a second example. The algorithm correctly identifies the change in reflectance between the sweatshirt and the jersey and correctly identifies the folds in the clothing as being caused by shading. There are some small shading artifacts in the reflectance image, especially around the sleeves of the sweatshirt, presumably caused by particular shapes not present in the training set. All of the examples were computed using ten non-linear filters as input for the AdaBoost gray-scale classifier.

5 Discussion

We have presented a system that is able to use multiple cues to produce shading and reflectance intrinsic images from a single image. This method is also able to produce satisfying results for real images. The most computationally intense steps for recovering the shading and reflectance images are computing the local evidence, which takes about six minutes on a 700MHz Pentium for a 256

$\times$ 256 image, and running the Generalized Belief Propagation algorithm. Belief propagation was used on both the x and y derivative images and took around 6 minutes to run 200 iterations on each image. The pseudo-inverse process took under 5 seconds.

The primary limitation of this method lies in the classifiers. For each type of surface, the classifiers must incorporate knowledge about the structure of the surface and how it appears when illuminated. The present classifiers operate at a single spatial scale, however the MRF framework allows the integration of information from multiple scales.

References

[1] H. G. Barrow and J. M. Tenenbaum. Recovering intrinsic scene characteristics from images. In *Computer Vision Systems*, pages 3–26. Academic Press, 1978.

[2] M. Bell and W. T. Freeman. Learning local evidence for shading and reflection. In *Proceedings International Conference on Computer Vision*, 2001.

[3] W. T. Freeman, E. C. Pasztor, and O. T. Carmichael. Learning low-level vision. *International Journal of Computer Vision*, 40(1):25–47, 2000.

[4] Y. Freund and R. E. Schapire. A decision-theoretic generalization of on-line learning and an application to boosting. *Journal of Computer and System Sciences*, 55(1):119–139, 1997.

[5] J. Friedman, T. Hastie, and R. Tibshirami. Additive logistic regression: A statistical view of boosting. *The Annals of Statistics*, 38(2):337–374, 2000.

[6] B. V. Funt, M. S. Drew, and M. Brockington. Recovering shading from color images. In G. Sandini, editor, *ECCV-92: Second European Conference on Computer Vision*, pages 124–132. Springer-Verlag, May 1992.

[7] D. Heeger and J. Bergen. Pyramid-based texture analysis/synthesis. In *Computer Graphics Proceeding, SIGGRAPH 95*, pages 229–238, August 1995.

[8] E. H. Land and J. J. McCann. Lightness and retinex theory. *Journal of the Optical Society of America*, 61:1–11, 1971.

[9] T. Leung and J. Malik. Recognizing surfaces using three-dimensional textons. In *IEEE International Conference on Computer Vision*, 1999.

[10] J. M. Rubin and W. A. Richards. Color vision and image intensities: When are changes material. *Biological Cybernetics*, 45:215–226, 1982.

[11] P. Sinha and E. H. Adelson. Recovering reflectance in a world of painted polyhedra. In *Fourth International Conference on Computer Vision*, pages 156–163. IEEE, 1993.

[12] K. Tieu and P. Viola. Boosting image retrieval. In *Proceedings IEEE Computer Vision and Pattern Recognition*, volume 1, pages 228–235, 2000.

[13] Y. Weiss. Deriving intrinsic images from image sequences. In *Proceedings International Conference on Computer Vision*, Vancouver, Canada, 2001. IEEE.

[14] J. Yedidia, W. T. Freeman, and Y. Weiss. Generalized belief propagation. In T. K. Leen, H. G. Diettrich, and V. Tresp, editors, *Advances in Neural Information Processing Systems 13*, pages 689–695, 2001.